

# Detection of elements beyond the Ba-peak in VLT+UVES spectra of post-AGB stars<sup>★</sup>

Maarten Reyniers and Hans Van Winckel<sup>★★</sup>

Departement Natuurkunde en Sterrenkunde, K.U.Leuven, Celestijnenlaan 200B, 3001 Leuven, Belgium

Received 14 May 2003 / Accepted 1 August 2003

**Abstract.** In this letter, we report on our successful systematic search for lines of elements beyond the Ba-peak in spectra of s-process enriched post-AGB stars. Using newly released atomic data from both the VALD database and the D.R.E.A.M. project, we could derive abundances for several elements heavier than europium for three objects, on the base of high quality VLT+UVES spectra. The abundances of these elements are of particular interest since they turn out to be powerful constraints for chemical evolutionary AGB models. Their high abundances indicate that, also in only moderately metal deficient AGB stars, production of lead is expected to be significant.

**Key words.** Line: identification – Stars: AGB and post-AGB – Stars: abundances – Stars: chemically peculiar

## 1. Introduction

There is now general consensus that the neutron nucleosynthesis in AGB stars is triggered by proton engulfment in the <sup>12</sup>C rich intershell (e.g. Busso et al. 1999). A significant <sup>13</sup>C-pocket is formed in a limited p/<sup>12</sup>C regime and the neutron irradiation occurs in radiative conditions (Straniero et al. 1995) during the interpulse period, when this <sup>13</sup>C pocket is consumed by  $\alpha$  captures producing <sup>16</sup>O and free neutrons. The dredge-ups associated with the thermal pulses during the AGB evolution will bring the enriched material to the stellar surface. There is, however, no consensus on the mechanisms of both the dredge-up processes and the partial mixing mechanism of protons in the intershell (e.g. Lugaro et al. 2003, and references therein).

The characteristics of the s-process nucleosynthesis are expected to be strongly dependent on the metallicity since the <sup>12</sup>C in the intershell is of primary origin, and thus largely independent on the initial <sup>12</sup>C content. Moreover, since the p/<sup>12</sup>C regime for which the s-process is expected to be active, is limited (Goriely & Mowlavi 2000), the uncertainties on the neutron irradiation are mainly from the extend of the proton engulfed zone in the intershell, and much less on the ad-hoc assumptions of the proton profile. In reduced environments, there are more neutrons available per iron seed, pushing the s-process to heavier elements. The prediction that in metal deficient ([Fe/H] < -1.0) stars, the production of Pb and Bi is expected to be significant (Gallino et al. 1998; Goriely & Mowlavi 2000)

was recently confirmed by the detection of such ‘lead-stars’ in extrinsic CH-stars by Van Eck et al. (2001).

The simple picture, in which the metallicity is the main parameter determining the s-process characteristics is, however, much less clear after the finding of a number of objects of the same metallicity, but with a large variety of s-process characteristics: s-process enriched objects of low metallicity ( $-3 < [\text{Fe}/\text{H}] < -1$ ) were found without the expected Pb enrichment (Aoki et al. 2001; Van Eck et al. 2003); and in less deficient post-AGB objects, large overabundances were found in which again a large spread in s-process efficiency was observed at similar metallicity (Van Winckel & Reyniers 2000; Reyniers et al. 2003).

In this paper we focus on a systematic search of the very heavy elements beyond the Ba-peak for the intrinsic post-AGB stars. The reason for this search is twofold: an accurate distribution of s-process overabundances is a prime tool to constrain the s-process nucleosynthesis and, second, in two, somewhat hotter post-AGB stars, hafnium ( $Z=72$ ) lines were tentatively detected, yielding a relatively large overabundance (Van Winckel & Reyniers 2000). Moreover, new atomic data for s-process elements beyond the Ba-peak became recently available, either through the VALD database (Kupka et al. 1999), or via the new D.R.E.A.M. project (<http://www.umh.ac.be/~astro/dream.shtml>). We used our high-resolution, high signal-to-noise (S/N) VLT+UVES spectra for this purpose. These spectra are described in detail in Reyniers et al. (2003). Here, we only note that they cover a spectral interval from 3745 Å to 10550 Å; that their resolving power varies between 55,000 and 60,000; and that the S/N is lying between 100 and 200 (depending on wavelength).

Send offprint requests to: Maarten Reyniers, e-mail: Maarten.Reyniers@ster.kuleuven.ac.be

<sup>★</sup> Based on observations collected at the European Southern Observatory, Paranal, Chile (ESO Programme 66.D-0171)

<sup>★★</sup> Postdoctoral fellow of the Fund for Scientific Research, Flanders

## 2. Systematic search

### 2.1. IRAS 06530–0213

We first concentrated on the spectrum of the heavily enriched IRAS 06530–0213 (Reyniers et al. 2003). We extracted all atomic data for lines of elements between gadolinium (Gd,  $Z = 64$ ) and platinum (Pt,  $Z = 78$ ) from either the VALD database or the D.R.E.A.M. project. By assuming an ad-hoc high abundance, we determined a list of the strongest lines of all elements using a model atmosphere of IRAS 06530–0213. The eventual presence of those lines was checked on the spectrum until the estimated strengths became too small to detect.

After that, the detected lines were thoroughly checked in four different ways: (1) Lines with a suspected profile (asymmetry, continuum placement, cosmic hit, end of CCD) were immediately discarded; (2) Lines were compared to the spectrum of HR 4656, a fast rotating ( $V \sin i \approx 210 \text{ km s}^{-1}$ ) Beta Cephei with spectral type B2IV, in order to check for telluric blending. Also the solar spectrum identification by Moore et al. (1966) was used for this purpose; (3) We also checked for possible diffuse interstellar bands (DIBs) in proximity of the line under study; (4) Blends are not always “visible” by a simple inspection of the line profile. Therefore, a final check was performed on the lines by the use of the VALD database. We extracted all lines from VALD in the immediate vicinity ( $\pm 1 \text{ \AA}$ ) of the line under study, and calculated the equivalent widths of all these extracted lines, using the abundances of IRAS 06530–0213. Such an exercise is highly necessary since it reveals sometimes strong blends (mostly from other s-process lines) which were not detected at first glance.

The final selection for IRAS 06530–0213 contains three lines of singly ionised gadolinium (Gd II,  $Z = 64$ ), two lines of singly ionised ytterbium (Yb II,  $Z = 70$ ) and two surprisingly strong lines of singly ionised lutetium (Lu II,  $Z = 71$ ). We also found one line of tungsten (W,  $Z = 74$ ), but the line is blended with a Sm II line. Nevertheless, we decided to derive a W abundance from this line by using spectrum synthesis (see Sect. 3). These lines are all shown in Fig. 1; their atomic data and equivalent widths can be found in Tab. 1.

### 2.2. IRAS 05341+0852

All lines detected in IRAS 06530–0213 were obviously also detected in the VLT+UVES spectrum of IRAS 05341+0852, but, as can be seen on Fig. 1 and Tab. 1, not all lines were used for an abundance determination since some are too blended with other s-process lines (e.g. the Gd II line at  $5092.249 \text{ \AA}$ ) or some are even too strong (e.g. the blended W II line at  $5104.432 \text{ \AA}$ ). On the other hand, three additional Gd II lines and one additional Yb II line were found suitable for an abundance determination. Plots and atomic data can again be found in Fig. 1 and Tab. 1 respectively.

### 2.3. IRAS 08143–4406

The line strengths of the trans-Ba elements detected in IRAS 06530–0213 and IRAS 05341+0852 are much smaller for IRAS 08143–4406, due to the less extreme enhancement of this object (Reyniers et al. 2003). Some lines are even untrace-

able (e.g. the Gd II line at  $5469.713 \text{ \AA}$ ). As a result, only three lines were found suitable for an abundance determination.

## 3. Abundances

Tab. 1 also contains the abundances derived from the selected lines. These abundances were calculated using Kurucz’ model atmospheres (Kurucz 1993) and the latest version (April 2002) of Sneden’s Stellar Line Analysis Program MOOG. Model parameters were taken from our earlier studies (IRAS 05341+0852: Van Winckel & Reyniers 2000; IRAS 06530–0213 and IRAS 08143–4406: Reyniers et al. 2003).

The W line at  $5104.432 \text{ \AA}$  does not fulfill the criteria mentioned above since it is blended with a Sm II line at  $5104.479 \text{ \AA}$ . In the case of IRAS 06530–0213, the total equivalent width of the blend is  $73.6 \text{ m\AA}$ , and the predicted contribution of the Sm II line is  $22 \text{ m\AA}$  (assuming  $\log \epsilon(\text{Sm}) = 2.09$ ). Spectrum synthesis with a macroturbulent broadening  $\xi_m = 19.5 \text{ km s}^{-1}$  (see Reyniers et al. 2003) yields a W abundance of  $\log \epsilon(\text{W}) = 3.04$ . Since it concerns an isolated blend, we deduced the abundance also without profile match solely on the equivalent width basis. This technique yields an abundance of  $\log \epsilon(\text{W}) = 2.92$ . We prefer to use this lower abundance since it is independent of the adopted  $\xi_m$ . However, one has to treat this abundance with caution since there might also be a blend present in the blue wing of the profile. We could not identify this blend, but it seems also present in the spectrum of the two other objects (see Fig. 1). In the case of IRAS 05341+0852, we did not derive a W abundance from the blended line at  $5104.432 \text{ \AA}$ , due to the relatively high contribution of the Sm II line in the blend ( $80.5 \text{ m\AA}$  assuming  $\log \epsilon(\text{Sm}) = 2.20$ ). Also for IRAS 08143–4406, the relative contribution is considered to be too high for a reliable abundance determination.

For Lu, hyperfine splitting (hfs) of the energy levels is expected. The Lu abundance was therefore deduced by spectrum synthesis. For the line at  $6221.890 \text{ \AA}$ , there are nine hfs components. Hfs A and B constants for the lower level were taken from Brix & Kopfermann (1952); for the upper level from Den Hartog et al. (1998). For the  $6463.107 \text{ \AA}$  transition, there are only three components, and the splitting is entirely due to the lower level, since for the upper level  $J = 0$ . Hfs constants for this level were also taken from Den Hartog et al. (1998). Relative strengths were calculated with the equations given in Condon & Shortly (1935). The effect of hfs on the Lu abundance determination is considerable. In the case of IRAS 06530–0213, the difference in abundance between a hfs and a non-hfs synthesis ( $\Delta \text{hfs}$ ) is  $-0.27 \text{ dex}$  for the  $6221.890 \text{ \AA}$  line, and  $-0.14 \text{ dex}$  for the  $6463.107 \text{ \AA}$  line. The effect is even larger for the cooler IRAS 05341+0852:  $\Delta \text{hfs} = -1.37$  and  $-0.48$  for the two lines respectively. For the hotter and less enhanced IRAS 08143–4406, hfs only affects the line profile, but not the equivalent width.

In Tab. 2 a summary of the final abundances is given. In order to compare these abundances with the solar ones, it should be checked that the solar abundances are based on the same sources of  $gf$  values as used in the present paper. This is, however, for several reasons not always straightforward. The orig-

**Table 1.** Atomic data and abundances of individual lines of s-process elements with  $Z > 63$ .

$\lambda$ (Å)	$\chi$ (eV)	$\log gf$	ref.	IRAS 05341		IRAS 06530		IRAS 08143	
				$W_\lambda$ (mÅ)	$\log \epsilon$	$W_\lambda$ (mÅ)	$\log \epsilon$	$W_\lambda$ (mÅ)	$\log \epsilon$
Gd II									
5092.249	1.727	-0.529	(1)	...	...	45.6	2.72	9.5	2.04
5108.903	1.659	-0.322	(1)	66.2	2.26	40.5	2.39	9.7	1.78
5357.794	1.157	-1.470	(1)	36.5	2.59	...	...	...	...
5469.713	1.102	-1.540	(1)	33.8	2.56	...	...	...	...
5733.852	1.372	-0.893	(1)	63.6	2.52	36.4	2.64	...	...
6080.641	1.727	-0.926	(1)	29.9	2.42	...	...	...	...
Yb II									
5352.954	3.747	-0.340	(2)	...	...	54.8	2.59	...	...
5651.988	3.747	-0.800	(2)	62.9	2.88	38.3	2.84	...	...
6489.298	4.153	-0.810	(2)	48.2	3.07	...	...	...	...
Lu II									
6221.890	1.542	-0.760	(3)	245.	1.58*	187.4	1.74*	42.1	0.97
6463.107	1.463	-1.050	(3)	230.	1.53*	157.9	1.78*	...	...
W II									
5104.432	2.355	-0.910	(4)	...	...	73.6	2.92 <sup>†</sup>	...	...

Refs. (1) Meggers et al. 1975 via Kurucz 1993 and VALD (2) Biémont et al. 1998 via D.R.E.A.M.

(3) Quinet et al. 1999 via D.R.E.A.M. (4) Clawson & Miller 1973 via Kurucz 1993 and VALD

\*abundance derived with spectrum synthesis (see text) <sup>†</sup>Sm blend taken into account (see text)

inal reference for the solar Gd abundance is Bergström et al. (1988) and it is based on eight Gd II lines, without overlap with the lines in this paper. However, the  $\log gf$  values of these eight lines are in our source (Meggers et al. 1975) somewhat lower (on average 0.14 dex) than the Bergström et al. values. This might be an indication that the Meggers et al. values are systematically too low and that the Gd abundances should be lowered by  $\sim 0.14$  dex to be consistent with the solar value. For Yb, the details of the solar abundance calculation are unfortunately lost (Grevesse, private communication). The solar Lu abundance is derived from the 6221 Å line (Bord et al. 1998; Den Hartog et al. 1998), with the same  $\log gf$  and hfs parameters as in this paper. Finally, the situation is less clear for W, since the solar value is derived from *neutral* W lines (Holweger & Werner 1982; Duquette et al. 1981). Moreover, there is a large discrepancy (0.42 dex) between the photospheric and the meteoritic value for this element, the photospheric being the most uncertain one (Grevesse & Sauval 1998).

#### 4. Discussion

To our knowledge, this is the first systematic search for trans-Ba elements in intrinsically enriched objects. Especially the detection of two strong Lu lines is astonishing, but an alternative identification was not found. Tomkin & Lambert (1983) reported the Lu II 6221.890 Å line to be blended in the classical Ba-star HR 774, but a blending species was, however, not given. We think this detection is real, and that the non-detection by previous authors is in fact a consequence of the lack of suitable line lists in the past, the time consuming procedure of a systematic approach in this matter and the lack of high S/N

**Table 2.** Final abundances of elements beyond the Ba-peak. For each ion, we list the number of lines  $N$ , the mean equivalent width  $\overline{W_\lambda}$ , the absolute abundance  $\log \epsilon$  (i.e. relative to H:  $\log \epsilon = \log X/H + 12$ ), the line-to-line scatter  $\sigma$  and the abundance relative to iron [el/Fe]. ss stands for spectrum synthesis, bl means corrected for blend. (Photospheric) solar abundances are taken from the review by Grevesse & Sauval (1998):  $\log \epsilon(\text{Gd})_\odot = 1.12$ ,  $\log \epsilon(\text{Yb})_\odot = 1.08$ ,  $\log \epsilon(\text{Lu})_\odot = 0.06$ ,  $\log \epsilon(\text{W})_\odot = 1.11$ .

ion	N	$\overline{W_\lambda}$	$\log \epsilon$	$\sigma$	[el/Fe]
IRAS 05341+0852					
[Fe/H] = -0.7, $T_{\text{eff}} = 6500$ K, $\log g = 1.0$					
Gd II	5	46	2.47	0.13	2.07
Yb II	2	56	2.98	0.13	2.62
Lu II	2	ss	1.56	0.04	2.22
IRAS 06530-0213					
[Fe/H] = -0.5, $T_{\text{eff}} = 7250$ K, $\log g = 1.0$					
Gd II	3	41	2.58	0.17	1.92
Yb II	2	47	2.71	0.18	2.09
Lu II	2	ss	1.76	0.03	2.16
W II	1	bl	2.92		2.27
IRAS 08143-4406					
[Fe/H] = -0.4, $T_{\text{eff}} = 7250$ K, $\log g = 1.5$					
Gd II	2	10	1.91	0.18	1.18
Lu II	1	42	0.97		1.30

spectra obtained with efficient spectrographs on large aperture telescopes.

As a final check for the identifications presented above, we compare the derived abundances with the predictions of the chemical evolutionary AGB models of the Torino group

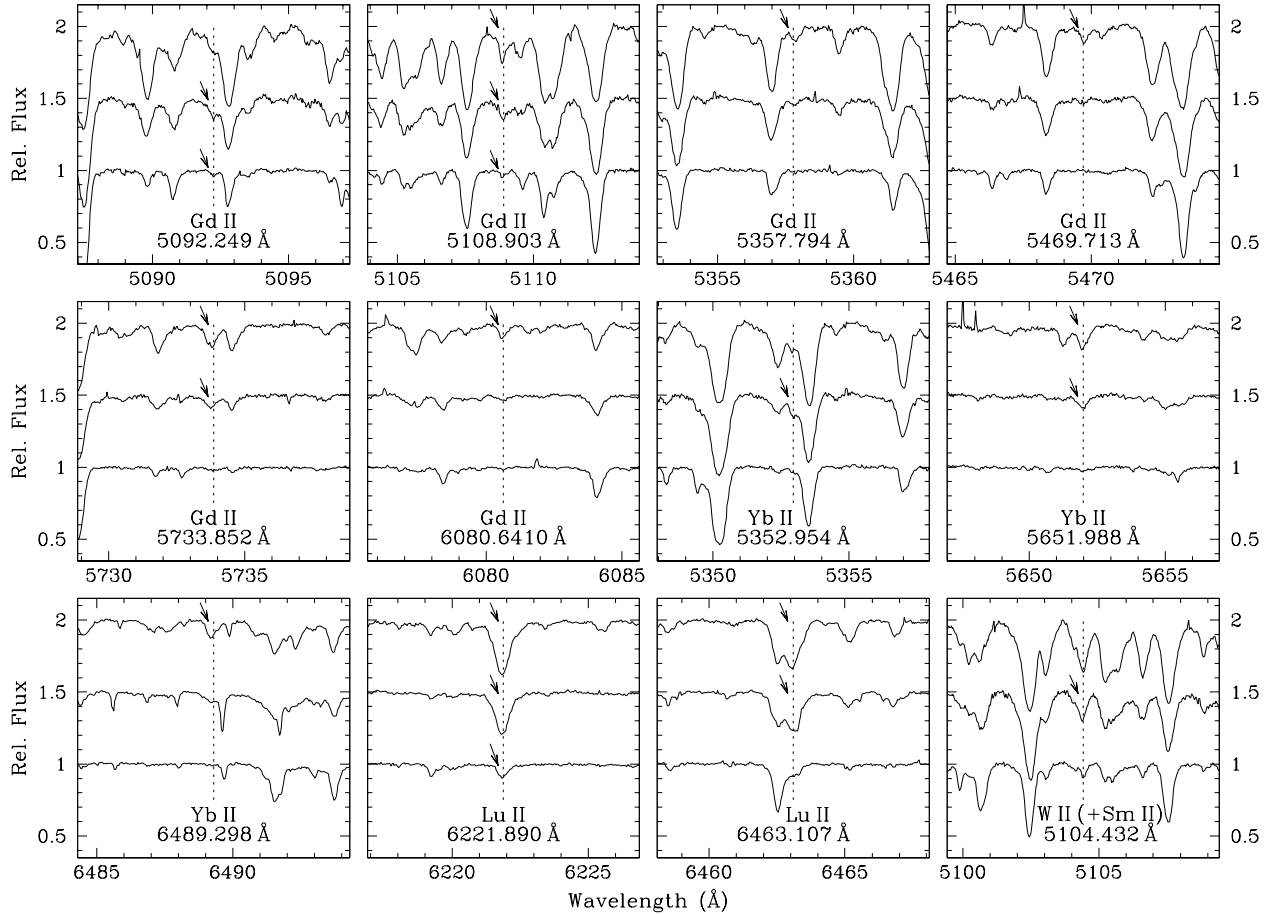


**Fig. 1.** Detection of lines from elements beyond the Ba-peak in the spectra of IRAS 05341+0852, IRAS 06530–0213 and IRAS 08143–4406. All these lines are intensively checked for blends, telluric pollution and DIB contamination (see text for details). From top to bottom are plotted: IRAS 05341+0852, IRAS 06530–0213 and IRAS 08143–4406. The spectral lines marked with an arrow are used for abundance determination.

(e.g. Gallino et al. 1998; Busso et al. 1999, 2001). These models are frequently used to fit observed abundances by adjusting the  $^{13}\text{C}$  pocket till the predicted and observed s-process distributions match. The fitting procedure, together with a more general discussion of the comparison, is described in detail in Reyniers et al. (2003). Here, we focus on the elements beyond the Ba-peak. In Fig. 2 we graphically compare the derived abundances with the best-fit model. The parameters of each model are given in the upper left corner; the initial mass is  $1.5 M_{\odot}$  for each model.

The predictions for the elements beyond the Ba-peak are consistent with the observed abundances. This is an additional argument strengthening the line identification for these elements. Only the Yb abundance of IRAS 05341+0852 is quite off the model curve (by +0.3 dex). More specifically, there is a large difference between the Yb abundance and the Lu abundance for IRAS 05341+0852, which is not predicted by the models. This difference is not seen in the abundances of IRAS 06530–0213, although three lines out of five are in common for these elements (see Tab. 1).

As can be seen from the comparison between two models with a different  $^{13}\text{C}$  pocket for IRAS 06530–0213, the abun-

dances of the very heavy s-process elements are most sensitive to the adopted  $^{13}\text{C}$  pocket. Hence, these elements (especially Hf and W) are ideally suited to discriminate between possible  $^{13}\text{C}$  pockets. Unfortunately, a Hf abundance is very difficult to obtain for these objects since it has only suitable lines in the blue, and the W abundance derived from the 5104.432 Å line depends on the adopted Sm abundance (see Sect. 3).

We conclude that we found trans-Ba abundances in strongly enriched post-AGB stars. Despite their difficult abundance determination, they are sensitive indicators for the strength of the neutron irradiation during the AGB interpulse phase. Note that also in these post-AGB stars with large overabundances of s-process elements beyond the barium stability peak, a strong overabundance of lead (Pb,  $Z = 82$ ) is expected. Unfortunately Pb has no suitable non-blended lines in the optical spectrum for these stars. Our detection of very heavy s-process elements indicate that also for moderate metallicities, Pb production is expected to be significant.

*Acknowledgements.* Roberto Gallino is warmly thanked for providing us with his latest model predictions, and for stimulating discussions. The anonymous referee is thanked for the suggestion of the importance of the Lu hyperfine splitting; Andrew McWilliam for his help

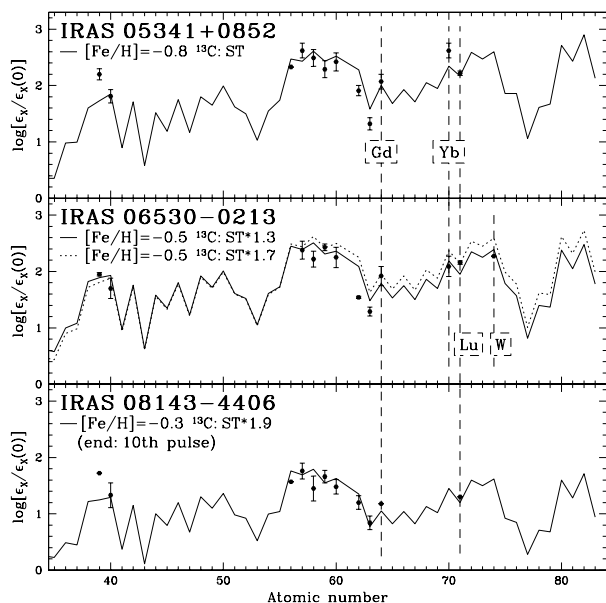


**Fig. 2.** Comparison of the observed abundances with the best fit Torino model predictions. The parameters of the adopted model are given in the upper left corner. Note that the specific model is obtained by fitting the Zr and La abundances (see Reyniers et al. 2003, for details), so *without* special attention to the very heavy s-process elements. The errorbars plotted on the figure are the line-to-line scatters that are given in Tab. 2. The actual error on an abundance is, however, in most cases considerably larger than this value, due to uncertainties in the atmospheric parameters, undetected blends, uncertain solar abundances, etc. . . One example is the solar abundance of W, for which there is a difference of 0.42 dex between the photospheric and the meteoritic value (Grevesse & Sauval 1998).

with the actual hfs calculation. Both authors acknowledge financial support from the Fund for Scientific Research - Flanders (Belgium). This research has made use of the Vienna Atomic Line Database (VALD), operated at Vienna, Austria, and the Database on Rare Earths At Mons University, operated at Mons, Belgium.

## References

Aoki, W., Ryan, S. G., Norris, J. E., et al. 2001, *ApJ*, 561, 346  
 Bergström, H., Biémont, E., Lundberg, H., & Persson, A. 1988, *A&A*, 192, 335  
 Biémont, E., Dutrieux, J.-F., Martin, I., & Quinet, P. 1998, *J. Phys. B: At. Mol. Opt. Phys.*, 31, 3321  
 Bord, D. J., Cowley, C. R., & Mirijanian, D. 1998, *Sol. Phys.*, 178, 221  
 Brix, P. & Kopfermann, H. 1952, in Landolt-Börnstein (ed.), *Zahlenwerte und Funktionen*, Vol. I, Part 5 (Springer-Verlag: Berlin), 1  
 Busso, M., Gallino, R., Lambert, D. L., Travaglio, C., & Smith, V. V. 2001, *ApJ*, 557, 802  
 Busso, M., Gallino, R., & Wasserburg, G. J. 1999, *ARA&A*, 37, 239  
 Clawson, J. E. & Miller, M. H. 1973, *JOSA*, 63, 1598

Condon, E. U. & Shortly, G. H. 1935, *The Theory of Atomic Spectra* (Cambridge University Press: London), 238  
 Den Hartog, E. A., Curry, J. J., Wickliffe, M. E., & Lawler, J. E. 1998, *Sol. Phys.*, 178, 239  
 Duquette, D. W., Salih, S., & Lawler, J. E. 1981, *Phys. Rev. A*, 24, 2847  
 Gallino, R., Arlandini, C., Busso, M., et al. 1998, *ApJ*, 497, 388  
 Goriely, S. & Mowlavi, N. 2000, *A&A*, 362, 599  
 Grevesse, N. & Sauval, A. J. 1998, *Space Science Reviews*, 85, 161  
 Holweger, H. & Werner, K. 1982, *Sol. Phys.*, 81, 3  
 Kupka, F., Piskunov, N., Ryabchikova, T. A., Stempels, H. C., & Weiss, W. W. 1999, *A&AS*, 138, 119  
 Kurucz, R. 1993, CD-ROM set, Cambridge, MA : Smithsonian Astrophysical Observatory  
 Lugaro, M., Herwig, F., Lattanzio, J. C., Gallino, R., & Straniero, O. 2003, *ApJ*, 586, 1305  
 Meggers, W. F., Corliss, C. H., & Scribner, B. F. 1975, *NBS Monograph*, 145  
 Moore, C. E., Minnaert, M. G. J., & Houtgast, J. 1966, *The solar spectrum 2935 Å to 8770 Å* (National Bureau of Standards Monograph 61)  
 Quinet, P., Palmeri, P., Biémont, E., et al. 1999, *MNRAS*, 307, 934  
 Reyniers, M., Van Winckel, H., Gallino, R., & Straniero, O. 2003, *A&A*, in preparation  
 Straniero, O., Gallino, R., Busso, M., et al. 1995, *ApJL*, 440, L85  
 Tomkin, J. & Lambert, D. L. 1983, *ApJ*, 273, 722  
 Van Eck, S., Goriely, S., Jorissen, A., & Plez, B. 2001, *Nat.*, 412, 793  
 —. 2003, *A&A*, 404, 291  
 Van Winckel, H. & Reyniers, M. 2000, *A&A*, 354, 135